International Journal of Scientific and Technological Research
ISSN 2422-8702 (Online)
Vol 1, No.10, 2015

Investigation of Microstructure, Physical and Thermal Properties of Al-Si-Sb Ternary Alloy

A. Aker (Corresponding author)
Department of Physics, Institute of Science and Technology, Erciyes University, Kayseri, Turkey
E-mail: aynuraker@hotmail.com

H. Kaya
Department of Science Education, Faculty of Education, Erciyes University, Kayseri, Turkey

Abstract
Al-12.6wt. %Si-2wt. %Sb alloy was directionally solidified with different growth rates (8,33-165,45 μm/s) at a constant temperature gradient of 8,04 K/mm using by Bridgman type growth apparatus. The values of interflake spacing (λ) was measured from transverse sections of the samples. The dependence of interflake spacing on the growth rate (V) was measured. Measurements of microhardness (HV), ultimate tensile strength (σ) and electrical resistivity (ρ) of the directionally solidified samples were carried out. The dependence of microhardness, ultimate tensile strength and electrical resistivity on growth rate (V) and interflake spacing (λ) was also analyzed. According to these results, it has been found that, for increasing values of V, the values of HV, σ and ρ are increase, for increasing values of λ, but values of HV, σ and ρ are descrease. Variations of electrical resistivity (ρ) for casting Al-Si-Sb alloy were also measured at the temperature in range 300–450 K. The enthalpy of fusion (ΔH) and specific heat (C_p) are calculated to be 282.60 J/g and 0.326 J/(g.K), respectively by means of differential scanning calorimeter (DSC) from heating trace during the transformation from liquid to solid. The results obtained in this work were compared with the similar experimental results in the literature.

Keywords: Al-Si-Sb alloy; Microstructures, Microhardness, Tensile Stress, Electrical resistivity, Enthalpy; Specific heat.

1. Introduction

Aluminum based alloys are widely employed in numerous automotive and industrial weight sensitive applications, such as gas turbine, aeronautics and space flight because of their low density and excellent cast ability. Actually, in most cases high-level mechanical properties are needed for industrial applications, so the performance of these alloys has been the subject of many micromechanical investigations [1]. Since the strength and hardness of alloys mainly depend on their microstructure, a lot of efforts have been made to refine the microstructure of the castings in order to enhance the mechanical properties of aluminum-based alloys. While research in the field of composite materials has yielded very exciting results, aluminum has remained at the centre of attention due to its attractive manufacturing costs, its extensive previous use in aircraft structures, and the availability of aluminum manufacturing facilities [2]. It is known that the mechanical properties of metallic materials are affected by their morphology. The mechanical properties of directionally solidified Aluminum alloys which are an important commercial material have been reported in several investigations [3-10] but the results differ from each other.

The automotive and aircraft industrial needs led to increasing application of Al-Si based alloys thanks to the great potential of these materials as replacements for heavier materials (steel, cast iron or copper) [11,12]. The Al–Si alloy system, which is characterized by high specific strength, excellent corrosion resistance, as well as good thermal and electrical conductivities, is widely used to supplant other alloys in the areas of transportation, packaging, construction, and machinery to achieve great weight reduction [13].

It is known that the mechanical and electrical properties of metallic materials are affected by theirs morphology. The mechanical and electrical properties of directional solidified Al–base alloys which are important commercial materials have been reported in several investigations [14, 15] but the results differ from each other. The microstructure evolution during solidification depends on the alloy characteristics and primarily is a function of the temperature profiles at the solidification interface. When a eutectic or near-eutectic alloy is solidified, the most frequently observed solid morphology is regular or irregular lamellar eutectic microstructures [16]. Microstructures are characterized by the microstructure parameters. Numerous solidification studies have been reported with a view to characterizing the microstructure parameters as a function of growth rate (V) [17, 18].
Thus, one of the aims of present work was to experimentally investigate the dependence of the flake spacings on the growth rate in the Al-Si-Sb ternary alloy and compare the results with the previous experimental results for similar alloys. The other aim of this work was to investigate the physical properties of the Al-Si-Sb ternary alloy such as microhardness, electrical resistivity, enthalpy of fusion, and the specific heat.

2. Experimental procedure

2.1. Sample production and microstructure observation

Al–12.6wt. %Si-2wt. %Sb samples were prepared by melting weighed quantities of Al, Si and Sb (purity>99.99%) in a graphite crucible placed into a vacuum melting furnace. After allowing time for melting homogeneously, the molten alloy was poured into seven graphite crucibles (250 mm in length, 4 mm inner diameter, and 6.35 mm outer diameter) in a hot filling furnace. Then, each specimen was positioned in a Bridgman-type furnace in a graphite cylinder (300 mm in length, 10 mm inner diameter, and 40 mm outer diameter). After stabilizing the thermal conditions under argon atmosphere, the specimen was grown by pulling downwards at a constant rate by means of a synchronous motor. Samples were solidified under steady-state conditions with a constant temperature gradient of 8.04 K/mm in a wide range of growth rates (8.33-165.45 μm/s).
The quenched sample was removed from the graphite crucible and cut into lengths typically of 8 mm. The longitudinal and transverse sections were ground flat with SiC paper (180, 500, 1000, and 2500 grit); then, grinded samples were cold mounted with epoxy-resin. After polishing, the samples were etched with 10vol% HF+90vol% H_2O for 10-15 s. After metallographic process, the microstructures of the samples were revealed. The microstructures of samples were photographed from transverse section with a LEO scanning electron microscopy (SEM) for different growth rates. Typical images of growth morphologies of directionally solidified Al-Si-Sb alloy were shown in Figure 1.

2.2. Measurement of solidification parameters and interflake spacing

The temperature in the specimen was measured by using three K-type insulated thermocouples (0.25 mm in diameter) fixed within the sample with spacing of 10-20 mm. All the thermocouples' ends were connected to a measurement unit consisting of a data-logger and a computer. The cooling rates were recorded by using the data-logger via the computer during growth. When the solid-liquid interface was at the second thermocouple, the temperature difference (ΔT) between the first and the second thermocouples was read from the data-logger record. The temperature gradient ($G = \Delta T/\Delta x$) for each sample was determined using the measured values of ΔT and the known value of Δx (distance difference of the thermocouples ends from buttom of the sample). The time (Δt) taken for the solid-liquid interface passed through the thermocouples separated by known distances (Δx) was read from data-logger record. Thus, the value of growth rate ($V=\Delta x/\Delta t$) for each sample was determined using the measured values of Δx and Δt. The measurements of λ were made from the photographs of microstructures with a linear intersection method [19-22]. The λ values on the transverse section were more reliable than the longitudinal section of the sample. So, the λ values were measured from transverse sections of the samples. So, the λ values were measured from transverse sections of the samples. The values of measured G, V and λ are given in Table 1 and Figures1-2.

2.3. Measurement of microhardness

The mechanical properties of any solidified material are usually determined by hardness test, tensile test, *etc*. Since true tensile strength testing of solidified alloys gave inconsistent results with a wide scatter due to the strong dependence on the surface quality of solidified sample, the mechanical

properties were monitored by hardness testing, which was one of the easiest and most straightforward techniques.

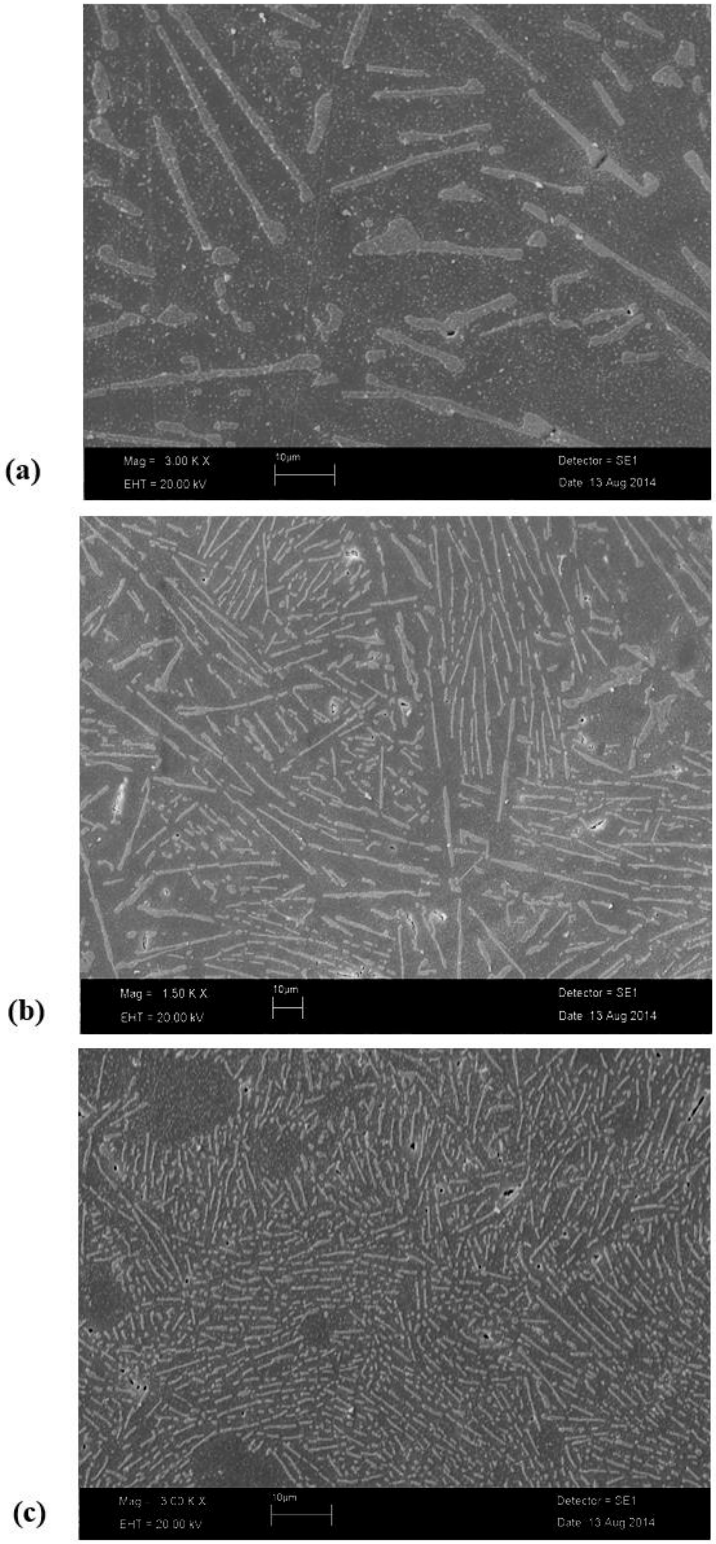

Figure 1. Micrographs of the directionally solidified Al-12.6wt% Si-2wt% Sb ternary alloy with a constant temperature gradient of 8.04 K/mm showing the eutectic microstructure: (a) V=8.33 µm/s, (b) 41.85 µm/s, (c) V=165.45 µm/s.

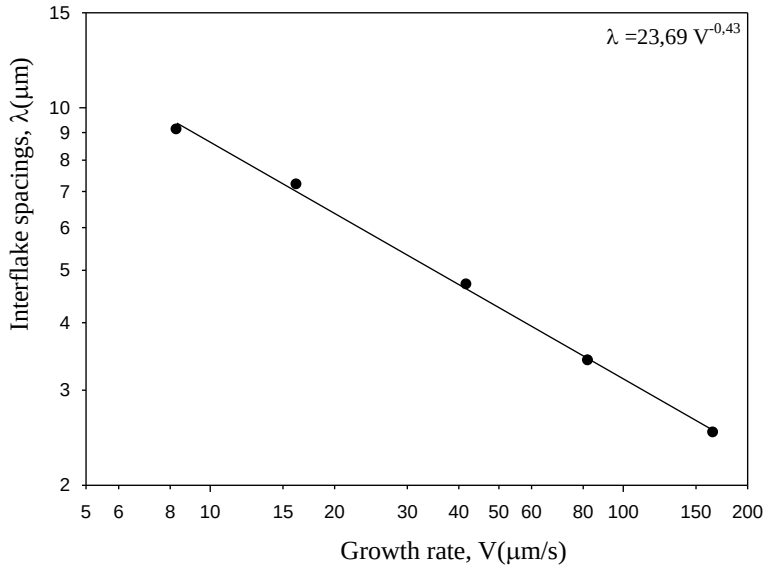

Figure 2. Variation of interflakes spacings a function growth rate

The Vickers hardness (HV) is the ratio of a load applied to the indenter to the surface area of the indentation. This is given by

$$HV = 2P\sin(\theta/2)/d^2 \quad (1)$$

Microhardness measurements in this work were carried out using a DuraScan hardness measuring test device using a 10-50 g load and dwell time of 10 s, giving a typical indentation depth of 40-60 μm, which was significantly smaller than the original solidified samples. Microhardness (HV) was measured for at least 300 different regions on transverse. The measured values of *HV* are also given in Table 1 and the variations of microhardness with the solidification processing parameters are plotted and given in Figures 3a and 3b.

Table 1. The values of solidification processing parameters, microstructures, microhardness, ultimate tensile strength and electrical resistivity for directionally solidified Al-Si-Sb ternary alloy, and relationships between them.

G **(K/mm)**	***V*** **(μm/s)**	***λ*** **(μm)**	***HV*** **(kg/mm^2)**	***σ*** **(MPa)**	***ρ*** **x10^{-5} (Ω mm)**
8.04	8.33	9.12	60.22	73.60	6.96
	16.23	7.24	63.30	80.20	7.35
	41.85	4.78	67.04	86.47	7.75
	82.35	3.42	69.80	102.10	8.20
	165.45	2.57	72.02	116.78	8.56
Relationships			**Constant (k)**		**Correlation coefficients (r)**

$\lambda=k_1V^{-0,46}$	$k_1=23,69(\mu m^{1,46}s^{-0,46})$	$r_1=0,998$
$HV=k_2V^{0,05}$	$k_2=80,73$ (kg $mm^{-2,05}sn^{0,05}$)	$r_2=0,996$
$HV=k_3\lambda^{-0,13}$	$k_3=32,08$ (kg $mm^{-1,87}$)	$r_3=0,993$
$\sigma=k_4V^{0,15}$	$k_4=148,84$(MPa $mm^{-0,15}$ $s^{0,15}$)	$r_4=0,980$
$\sigma=k_5\lambda^{-0,34}$	$k_5=159,26$(MPa $mm^{0,34}$)	$r_5=0,984$
$\rho=k_6V^{0,06}$	$k_6=9,69\Omega\mu m^{0,94}s^{0,06}$	$r_6=0,998$
$\rho=k_7\lambda^{-0,15}$	$k_7=3,36\Omega mm^{1,15}$	$r_7=0,996$

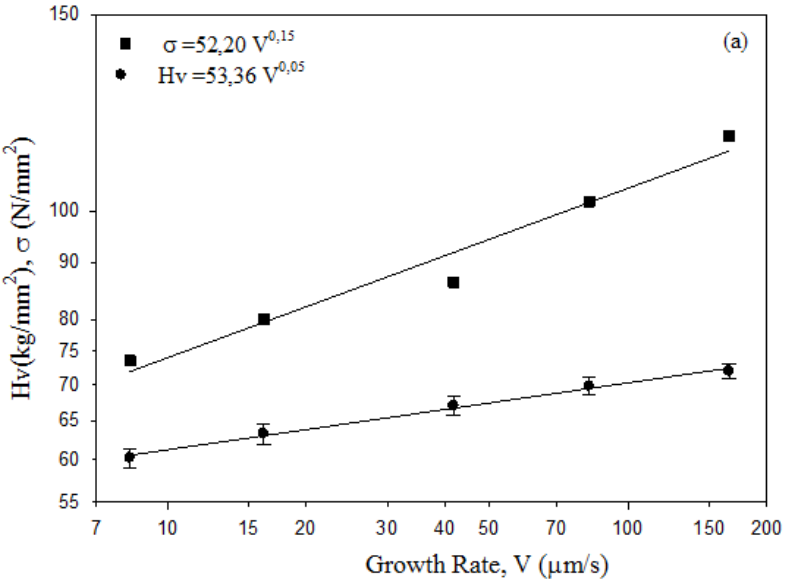

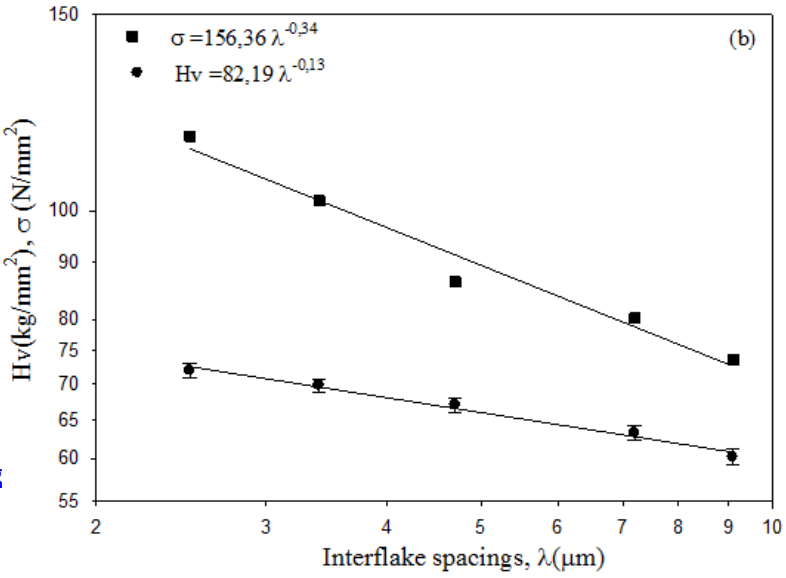

Figure 3. (a) Variation of microhardness, Hv, and tensile strength σ, as a function growth rate
(b) Variation of microhardness, Hv, and tensile strength σ, as a function interflakes spacings

2.4. Determination of ultimate tensile strength (UTS)

Another aim of this work was to obtain the relationship between ultimate tensile strength (UTS), the growth rate and interflake spacings in the Al-Si-Sb ternary alloy.

The tests of tensile strength were performed at room temperature at a strain rate of 10^{-3} s^{-1} with a ***Shimadzu AG-XD universal testing machine***. The data collected from the tensile test can be analysed using the following formula to determine the strength (σ)

$$\sigma=F/A \quad (2)$$

where σ is the strength in N /mm^2 (or MPa), F is the applied force (N), A is the original cross sectional area (mm^2) of the sample. The round rod tensile samples with diameter of 4 mm and gauge length of 50 mm were prepared from directionally solidified rod samples with different growth rates (V=8.33-165.45 μm/s) at a constant G (8.04 K/mm).
The tensile axis was chosen parallel to the growth direction of the sample. UTS (σ) values of Al-Si-Sb alloy are shown in Figures 3a and 3b for V and λ values.

2.5. Measurement of electrical resistivity

Another purpose of this investigation was to obtain the relationships among the growth rate, dendritic microstructures and electrical resistivity for the Al-Si-Sb samples. The electrical resistivity of directionally solidified samples was measured by the d.c. four-point probe method. The four-point probe method is the most widely used technique for electrical profile measurement of materials. The method has proven to be a convenient tool for the resistivity measurement In this method, the material's resistivity can be expressed as,

$$\rho = RCF \frac{V}{I} \quad (3)$$

where RCF is resistivity correction factor, *V* is the potential difference measured across the probes and I is the current through the probes. The geometry of the sample determines the correction factors that must be used, additionally the position of the probes on the sample and the spacings between the probes. The need for correction factors is caused by the proximity of a boundary which limits the possible current paths in the sample. The number of RCF is calculated by diameter of sample divided by probe **s**pacing (probe spacing being the distance between any two adjacent probes). In this study, a 4mm diameter sample probed with a four point probe with 1mm tip spacing would have a correction factor of 0.65.
When a constant current was applied on the sample with a *Keithley 2400* sourcemeter the potential drops on the samples were measured with a *Keithley 2700* multimeter connected to a computer. Platinum wire, 0.5 mm in diameter was used to be the probes of current and potential.
Two of the probes are used to source current and the other two probes are used to measure voltage, using four probes eliminates measurement errors due to the probe resistance, the spreading resistance under each probe, and the contact resistance between each metal probe and material [23]. The sizes of samples were measured by using a digital micrometer, has an accuracy of 1 μm. The error in the electrical resistivity measurements is calculated about 5 %. This error is due to current, voltage and temperature measurements.

2.6. Determination of enthalpy and specific heat

The enthalpy of fusion (ΔH) and the specific heat (C_p) of Al-Si-Sb alloy were determined because they are very important parameters for industrial applications. Differential scanning calorimeter (DSC) thermal analysis (Perkin-Elmer Diamond model) was performed at 300-1200 K with a heating rate of 10 K/min under a constant stream of nitrogen at atmospheric pressure.

A reference material (a sapphire disk) was used in determining specific heat. This reference data was used to "correct" sample data at every temperature. The size of the signal which was used to calculate the specific heat was proportional to the heating rate, so it follows that faster heating rates will produce larger signals, which will give more accurate data. However, if the heating rate was too high, the temperature gradients in the sample would be large and this may introduce other errors in the measurement. It was normal to use heating rates between 5 and 20 K/min. The heating rate in this study was 10 K/min, which was mostly recommended.

The difference between the sample curve and the baseline curve was measured in milliwatts and converted to specific heat as follows,

$$Cp=(dQ/dt)(1/MR) \quad (4)$$

where dQ/dt is the heat flow; M (g) the mass of the sample; and R the heating rate, K/min.

The DSC curve obtained for Al-Si-Sb alloy is shown in Figure 6. A sharp peak is clearly observed for melting process, as shown in Figure 6. The enthalpy of fusion (ΔH) and specific heat (C_p) were calculated as the area under the peak by numerical integration.

3. Results and discussion

3.1. Effect of growth rate on the inter flake spacing

Variations of inter flake spacings (λ) with the growth rate (V) at a constant G (8.04 K/mm) is given in Figure 2 and Table 1. The variation of λ versus V can be given the proportionality equation as,

$$\lambda = kV^{-n} \quad (5)$$

where k is a constant and n an exponent value of growth rate. The relationships between the flakes spacing and growth rates were determined as. $\lambda=23{,}69\ V^{-0,43}$ by using linear regression analysis. The exponent value 0.43 is in good agreement with the range values of 0.39-0.47 obtained by different researchers [6,10,14,17,24,25].

3.2. Dependence of microhardness and ultimate tensile strength on growth rate

One of the purposes of this investigation is to obtain the dependence of HV on V and λ. It can be seen from Table 1 that an increase in the temperature gradient and growth rate leads to an increase in the microhardness. Dependence of the HV on the V and λ were determined by using linear regression analysis and the relationship between them can be expressed by the following equations as,

$$HV = k_2 V^b \quad (6)$$

$$HV = k_3 \lambda^c \quad (7)$$

where k_2 and k_3 are constant, b and c are the exponent values of the growth rate and flake spacing, respectively. As can be seen from Figures 3a and 3b, the microhardness values increase with the increasing V values and decreasing with the increasing λ values.

Linear regression analysis yields

$$HV = 80{,}73V^{0,05} \quad (8)$$

$$HV = 32{,}08\ \lambda^{-0,13} \quad (9)$$

The average exponent values of V and λ for HV in the directionally solidified Al-Si-Sb alloy were found to be 0.05 and 0.13, respectively in this work. These exponent values relating to V and λ obtained in present work is generally in a good agreement with the exponent values obtained in previous experimental works [17, 21-22, 26] under similar solidification conditions.

Typical strength-strain curves of Al-Si-Sb alloy are shown in Figure 3 for V and λ values. As can bee seen from Figure 3, ultimate tensile strength (UTS, σ) values are increased with increasing V, but eutectic spacings values are increased ultimate tensile strength decreased.

Figures 3a and 3b show the variation of the UTS (σ) with the growth rate (V) and interflake spacings. The dependence of σ on V and λ, can be represented as,

$$\sigma = k_4 V^d \quad (10)$$

$$\sigma = k_5 \lambda^e \quad (11)$$

As can be seen from Figure 3a, the values of σ increase with increasing growth rate. The exponent value of V is found to be 0.16 and value of λ is found to be 0.37 (Figure 3b).

3.4. Electrical properties of Al-Si-Sb ternary alloy

It can be seen from Table 1, temperature gradient and growth rate lead to an increase in the electrical resistivity. Dependence of the electrical resistivity on growth rate and interflake spacings can be expressed as

$$\rho = k_6 V^f \quad (12)$$

$$\rho = k_7 \lambda^g \quad (13)$$

where k_6 and k_7 are constants which can be experimentally determined and given in Table 1. The value of the exponent relating to the growth rate and eutectic spacings were obtained to be 0.06 and 0.15, respectively (Figure 4).

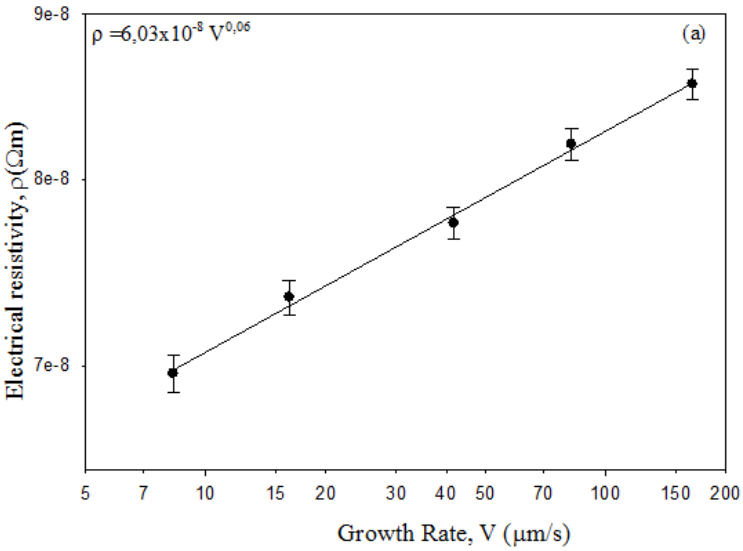

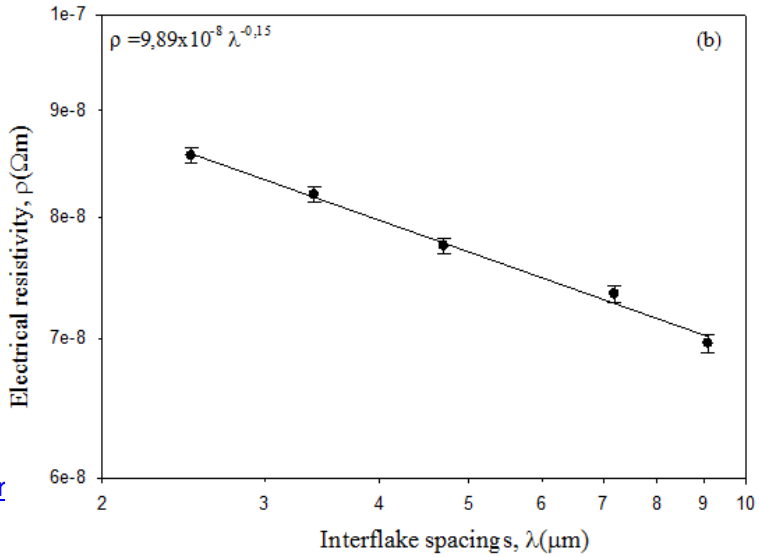

Figure 4. (a) Variation of electrical resistivity, as a function growth rate
(b) Variation of electrical resistivity, as a function interflake spacings

The variation of electrical resistivity with the temperature in the range of 300–450 K was measured (see Figure 5). It is observed that an increase in the temperature (300–450 K) values lead to increase in the electrical resistivity values (6.39–9.92)×10^{-5} Ωmm.

As can be seen from Figure 5 the electrical resistivity values (6.39–9.92×10^{-5} Ωmm) in this work are some higher than the values (2.75–8.75×10^{-5} Ωmm) for pure aluminum, and smaller than the values (41.3–110×10^{-5} Ωmm) for pure antimony [27].

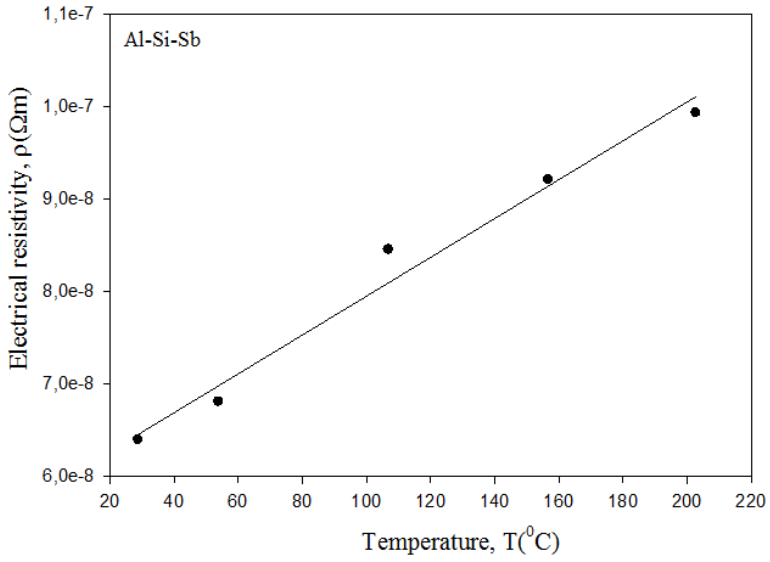

Figure 5. Variation of electrical resistivity as a function temperature for Al-Si-Sb ternary alloy.

3.5 The thermal properties of Al-Si-Sb alloy

The Al–Si-Sb alloy was heated with a heating rate of 10 K/min from room temperature to 1200 K by using a ***Perkin Elmer Diamond*** model DSC and the heat flow versus temperature is given in Figure 6. As can be seen from Figure 6, the melting temperature of Al-Si-Sb eutectic was found to be 866.37 K. The values of the enthalpy of fusion and the specific heat were also calculated to be 282.60 J/g and 0.326 J/(g.K) respectively from the graph of the heat flow *vs*. temperature. The recommended values of the enthalpy of fusion for pure Al, Si, Sb and Al-Si eutectic are 396.96 J/g, 297.83 J/g, 161 J/g and 468.2 J/g respectively, and also, the specific heat values for pure Al, Si, Sb and Al-Si eutectic are 0.879 J/gK, 0.210 J/gK, 0.21 J/gK and 0.0563 J/gK, in respectively [28, 29] at the melting temperature. The

ΔH value (282.60 J/g) is smaller and the Cp values (0.326 J/gK) is same higher than the values of pure Al, Si, Sb and Al-Si eutectic.

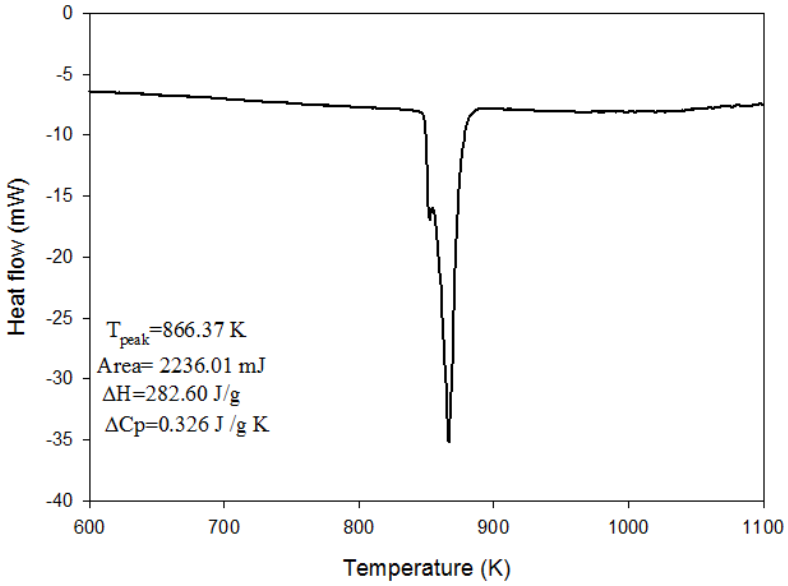

Figure 6. Heat flow curve vs. the temperature for Al-Si-Sb ternary alloy at heating rate of 10 K/min.

4. Conclusions

The principal results in this work can be summarized as follows;

1. Experimental observations show that the values of flake spacings (λ) decreases as growth rate (V) increases. The relationships between λ and V have been obtained to be $\lambda=23.69\ V^{-0.43}$.
2. It was found that the values of HV increase with increasing the values of V, but the values of the HV descrease with increasing the values of λ. The establishment of the relationships among HV, V and λ can be given as $HV=53.36V^{0.15}$ and $HV= 82{,}19\ \lambda^{-0.13}$.
3. The experimental expressions correlating the values of *ultimate tensile strength* (σ) with the values of V and λ shows that the values of the tensile stresses increase with increasing the values of V and the values of the tensile stresses descrease with increasing the values of λ. The establishment of the relationships among stresses (σ) and solidification parameters (V and G) can be given as $\sigma=52.20(V)^{0.15}$ and $\sigma=156.56(\lambda)^{-0.34}$.
4. Experimental results show that the values of electrical resistivity (ρ) increases with increasing V values, but the values of ρ descrease with increasing the values of λ. The relationships between ρ and V and λ have been obtained to be $\rho=6.03\times10^{-8}\ (V)^{0.06}$ and $\rho=9.89\times10^{-8}\ (\lambda)^{-0.15}$.
5. The electrical resistivity of Al-Si-Sb alloy increases $(6.39–9.92)\times10^{-5}$ Ωmm with increasing temperature (300-450 K).
6. From the plot of heat flow *vs.* temperature, the melting temperature, enthalpy of fusion, and specific heat are found to be 866.37 K, 282.60 J/g and 0.326 J/(g.K), respectively.

References

[1] Yang, F., Peng, L., and Okazaki, K. 2004. Microindentation of aluminum. Met.Mat. Trans. 35A: p.3323.

[2] Ping Wu, S., Liu, D.R., Guo, J.J., Su, Y.Q. and Fu, H. Z. 2007. Influence of process parameters on CET in Ti–Al alloy ingot with consideration of shrinkage cavity formation: A computer simulation. J. Alloys and Comp. 441: p. 267.

[3] Yang, F., Peng, L. and Okazaki, K. 2004. Microindentation of aluminum, Met. Mat. Trans. A35: p.3323.

[4] Goulart, P. R., Spinelli, J. E., Osório, W. R., Garcia, A. 2006. Mat. Sci. Eng. A 421: p.245.

[5] Gögebakan, M., Uzun, O., Karaaslan, T., Keskin, M. 2003. Rapidly solidified Al–6.5 wt.% Ni alloy, J. Mat. Proc. Tech. 142: p.87.

[6] Kaya, H., Gündüz, M., Çadırlı, E., Uzun, O., 2004. Effect of growth rate and lamellar spacing on microhardness in the directionally solidified Pb-Cd, Sn-Zn and Bi-Cd eutectic alloys, J.Mat. Sci. 39: p.6571.

[7] Kaya H, Çadırlı E, Gündüz M, Ülgen A. 2003. Effect of the temperature gradient, growth rate and the interflake spacing on the microhardness in the directionally solidified Al-Si eutectic alloy, *J.Mat.Eng Perf.* 12: p. 544.

[8] Kaya, H., Çadırlı, E., Böyük, U., and Maraşlı, N. 2008. Variation of microindentation hardness with solidification and microstructure parameters in the Al based alloys, Appl. Surf. Sci., 255: p.3071.

[9] Engin, S., Böyük, U., Kaya, H., Maraşlı, N. 2011. Directional solidification and phiycsal properties measurements of the zinc-aluminum eutectic alloy, I. J. Min, Met Mat, 18(6): p. 659.

[10] Böyük U., Maraşlı N., Çadırlı E. Kaya H. Keşlioğlu K. 2012. Variations of microhardness with solidification parameters and electrical, resistivity with temperature for Al-Cu-Ag eutectic alloy, Current Applied Physics 12: p.7.

[11] Wang, E. R., Hui, X. D., Wang, S. S., Zhao, Y. F., Chen, G. L. 2010. Improved mechanical properties in cast Al-Si alloys by combined alloying of Fe and Cu. Materials Science and Engineering A, 527: pp. 7878-7884.

[12] Samuel, A. M., Samuel, F. H., Doty, H. W. 1996. Observation on the formation ß-Al5FeSi phase in 319 type Al-Si alloys. Journal of Materials Science, 31: pp. 5529-5539.

[13] Lu L., Dahle A.K., 2006. Mater. Sci. Eng. A, 435–436: pp. 288–296.

[14] Kaya H. 2012. Dependency Of Electrical Resistivity On The Temperature And Composition Of Al-Cu Alloys. Materials Research Innovations, 16 (1): pp. 224-229,

[15] Kaya H., Çadirli E., Ülgen A. 2011. Investigation Of The Effect Of Composition On Microhardness And Determination Of Thermo-Physical Properties In The Zn-Cu Alloys, Materials& Design, 32: pp. 900-906.

[16] Trivedi R. and Kurz W. 1994. Int. Mat. Rev. 39: pp.49.

[17] Yilmazer M. İ., Kaya H., Aker A., Engin S. 2013. Influence Of The Growth Rate On Physical Properties In The Aluminum-Antimony Eutectic Alloy. International Journal of Materials Engineering and Technology, 9: pp. 59-76.

[18] Aker A., Kaya H. 2013. Measurements of Microstructural, Mechanical, Electrical and Thermal Properties of an Al-Ni Alloy, International Journal of Thermophyscics, 34 (1): pp. 267-283.

[19] Ourdjini, A., Liu, J. and Elliott, R. 1994. Eutectic spacing selection in the Al-Cu system, Mater. Sci. Tech.-Lond. 10: p.312.

[20] Kaya, H. Çadırlı, E. and Gündüz, M. 2007. Eutectic growth of unidirectionally solidified bismuth-cadmium alloy. J. Mat. Process Tech., 183: p.310.

[21] Kaya, H., Çadırlı, E. and Gündüz, M. 2003. Effect of growth rates and temperature gradients on the spacing and undercooling in the broken-lamellar eutectic growth (Sn-Zn eutectic system). J. Mat. Eng. Perf., 12(4): p.456.

[22] Sergeev, A. and Mitin, V. 2000. Electron-phonon interaction in disordered conductors: Static and vibrating scattering potentials*Phys. Rev.B,* 61: p.6041.

[23] Boekelheide, Z., Cooke, D.W., Helgren, E. and Hellman, F. 2009. Resonant impurity scattering and electron-phonon scattering in the electrical resistivity of Cr thin films. Phys. Rev. B, p. 80134426.

[24] Rudnev V., Loveless D., Cook R. Black M. 2003. Handbook of Induction Heating, Markel Dekker Inc. New York. p. 119.

[25] Hultgren, R., Orr, R. L., Anderson, P.D. and Kelley, K.K. 1963. Selected Values of Thermodynamic Properties of Metals and Alloys, (University of California, Berkeley: Wiley. p.318-322.

[26] Fan, J., Li, X., Su, Y., Guo, J. and Fu, H. 2010. The microstructure parameters and microhardness of directionally solidified Ti-43Al-3Si alloy. Journal of Alloys and Compounds, 506**:** 593-599.

[27] Steinbach, S., Ratke L., 2007. Experimental study on interaction of fluid flow and solidification in Al-Si-Cu alloys**.** International Journal of Cast Metals Research. 20: 140-144.

[28] Böyük, U. 2012. Physical and mechanical properties of Al–Si–Ni eutectic alloy. Metals and Materials International. 18, (6): 933-938.